

Longitudinal Magnetic Excitations in Classical Spin Systems

Alex Bunker* and D. P. Landau

Center for Simulational Physics, University of Georgia, Athens, Georgia 30602-2451

(Received 4 October 1999)

Using spin dynamics simulations we predict the splitting of the longitudinal spin-wave peak in all antiferromagnets with single site anisotropy into two peaks separated by twice the energy gap at the Brillouin zone center. This phenomenon has yet to be observed experimentally but can be easily investigated through neutron scattering experiments on MnF_2 and FeF_2 . We have also determined that for all classical Heisenberg models the longitudinal propagative excitations are entirely multiple spin wave in nature.

PACS numbers: 75.30.Ds, 75.10.Hk, 75.40.Mg

While the transverse component of the dynamic structure factor is well understood, including the phenomenon of multiple transverse excitations [1], the mechanism for longitudinal excitations in high spin magnets with weak to moderate anisotropy, like MnF_2 , FeF_2 , RbMnF_3 , EuO , and EuS , is not completely understood. There are conflicting theoretical predictions [2,3] and experimental results of limited resolution [3–5]; however, the spin dynamics simulation technique is able to analyze both the transverse and longitudinal components of the dynamic structure factor for simple classical Heisenberg models. This is true in both the hydrodynamic and critical temperature regimes and, unlike mode coupling theory, the accuracy of our results can be improved continuously through the use of more computer time. Indeed using high speed supercomputers we have already achieved considerably higher precision than existing experimental results.

The above materials all have spin values ($S \geq 2$) which are large enough to be effectively described by the classical limit, $S \rightarrow \infty$, and bilinear exchange interactions between nearest, and in some cases second neighbor atoms on simple lattice structures. RbMnF_3 is a simple cubic (sc) antiferromagnet, MnF_2 and FeF_2 are body centered cubic (bcc) anisotropic antiferromagnets with weak and moderate anisotropy, respectively, and EuO and EuS are ferromagnets. The degree of anisotropy in EuO , EuS , and RbMnF_3 is negligible. While for EuO and EuS , and to a lesser extent MnF_2 and FeF_2 , the second neighbor interactions are not negligible, a qualitative understanding of the magnetic dynamics can still be obtained through a model with only nearest neighbor interactions.

We performed our simulation on the isotropic sc Heisenberg magnet with both ferro- and antiferromagnetic bilinear interactions and the anisotropic bcc Heisenberg antiferromagnet. The Hamiltonian for our model is given by

$$\mathcal{H} = J \sum_{\langle \mathbf{r}\mathbf{r}' \rangle} \mathbf{S}_{\mathbf{r}} \cdot \mathbf{S}_{\mathbf{r}'} - D \sum_{\langle \mathbf{r} \rangle} (\mathbf{S}_{\mathbf{r}}^z)^2, \quad (0.1)$$

where $\mathbf{S}_{\mathbf{r}}$ is a three-dimensional classical spin of unit length, $\langle \mathbf{r}\mathbf{r}' \rangle$ is a nearest neighbor pair, and D is the uniaxial single-site anisotropy term. We determined the

dynamic structure factor in the [100], [110], and [111] reciprocal lattice directions. For the antiferromagnetic case we have made the transformation $q \rightarrow q + Q$ where Q is the Brillouin zone boundary in the [111] direction.

We have used the spin dynamics simulation technique, which has been developed in previous work [6,7], to calculate the dynamic structure factor. The spin dynamics simulation technique involves the creation of an equilibrium distribution of initial configurations using the Monte Carlo (MC) technique which are then precessed through constant energy dynamics to yield the space-time correlation function from each configuration. These are averaged together and Fourier transformed to obtain a result for the dynamic structure factor. By including more initial configurations the accuracy can be improved indefinitely. We have used periodic boundary conditions and studied lattices of linear sizes of $L = 12$ and $L = 24$. The critical temperatures were determined using the fourth order cumulant crossing technique [8] for the anisotropic systems, and T_c is already accurately known for the isotropic Heisenberg model [9]. Anisotropy value $D = 0.0591$ was used for MnF_2 to match the experimentally determined [10] degree of anisotropy.

For all these models we performed the simulation at temperature $T = 0.5T_c$, low enough to be completely outside the critical regime but not too low for the MC simulation to produce an equilibrium distribution of configurations. We also studied $T = 0.8T_c$ and $T = 0.9T_c$ for the isotropic ferromagnet to investigate the approach to the critical regime. The results from the higher temperature simulations were convoluted with a Gaussian resolution function of width δ_ω to minimize effects due to the finite time cutoff. For the isotropic case we used a distribution of 1000 initial configurations for $L = 12$ and 200 configurations for $L = 24$, and for the anisotropic case we used 6000 configurations for $L = 12$ and 400 configurations for $L = 24$. A smaller number of configurations was used for $L = 24$ due to limits of computer time.

For the longitudinal component of the dynamic structure factor in the ferromagnetic case we observed many excitation peaks, as seen in Fig. 1; however, a different set is present for the $L = 12$ and $L = 24$ lattice sizes at the same \mathbf{q} value. We conjecture that these excitations are

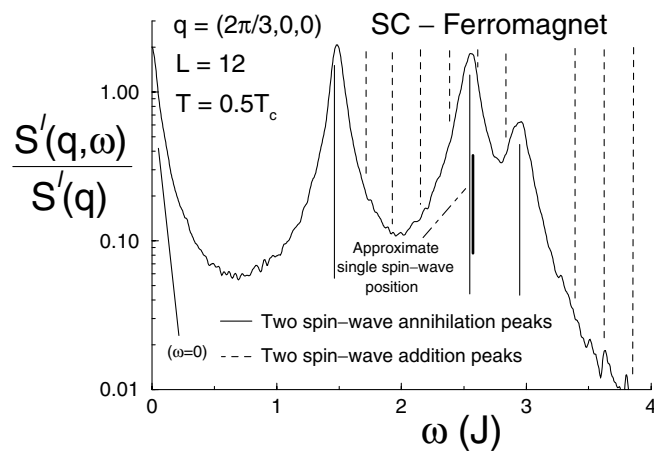


FIG. 1. The longitudinal component of the dynamic structure factor for the isotropic sc ferromagnet vs frequency. The predicted positions of the two-spin-wave peaks are superimposed on the graph of the dynamic structure factor. Note that a logarithmic scale has been used for the dynamic structure factor.

two-spin-wave peaks since due to finite lattice size effects the frequencies of the peaks will be limited to certain values which will be different for different lattice sizes. In order to test this hypothesis we need to be able to predict the expected positions of the two-spin-wave peaks. This requires that we obtain an approximate estimate for the general form of the dispersion curve at the temperature at which the simulation is performed, i.e., $\omega(\mathbf{q})$ at all points on the reciprocal lattice.

The dispersion curve at $T = 0$ will be given by the linear spin-wave dispersion curve, $\omega(\mathbf{q})$. We found that for temperatures below $T = 0.5T_c$ the functional form of the dispersion curve is maintained, multiplied by the factor $D(T)/D(0)$, where $D(T)$ is the spin-wave stiffness coefficient. At $T = 0.5T_c$ the functional form diverges only slightly in the high q region where the prediction is at a lower ω value than the actual result, however in the low q region this approximation is still valid. Now that we have determined that the linear spin-wave result multiplied by the factor $D(T)/D(0)$ is a good approximation to the dispersion curve at $T = 0.5T_c$ in the low q region, we can estimate the spin-wave frequency in all directions in reciprocal lattice space, not just those we have measured.

All two-spin-wave creation peaks will be at frequency

$$\omega_{ij}^+(\mathbf{q}_i \pm \mathbf{q}_j) = \omega(\mathbf{q}_i) + \omega(\mathbf{q}_j) \quad (0.2)$$

and the spin-wave annihilation peaks will thus be at frequency

$$\omega_{ij}^-(\mathbf{q}_i \pm \mathbf{q}_j) = \omega(\mathbf{q}_i) - \omega(\mathbf{q}_j), \quad (0.3)$$

where \mathbf{q}_i and \mathbf{q}_j are the wave vectors of the two spin waves which comprise the two-spin-wave excitation. As shown in Fig. 1, for the isotropic ferromagnet we see a near perfect match of peaks in $S(\mathbf{q}, \omega)$ and the predicted positions of the two-spin-wave annihilation peaks, clearly indicating that

the excitations in the longitudinal component are due to two-spin-wave annihilation.

For the anisotropic antiferromagnet the approximation of the dispersion curve from a measurement of $D(T)$ is inaccurate since the actual dispersion curve does not follow the functional form of the zero temperature dispersion curve. Instead we identified a set of two-spin-wave annihilation and creation peaks which involve spin waves exclusively in the reciprocal lattice directions which we measured. Plotting the expected frequencies of these two-spin-wave peaks we see a good match between the longitudinal spin waves and the expected values for both the annihilation and creation peaks. This result for weak anisotropy (MnF_2) is shown in Fig. 2. Note that no trace of a peak is seen at the location of the single spin-wave peak in the transverse component. We see, as expected, the presence of both creation and annihilation spin-wave peaks for the isotropic antiferromagnet as well.

The two-spin-wave peaks where one of the single spin waves of which they are made up has the lowest \mathbf{q} are the most intense. This is to be expected since the lower \mathbf{q} single spin waves are more intense themselves. As the temperature rises the two-spin-wave peaks broaden. For the antiferromagnetic case, where the longitudinal and transverse components cannot be separated, as T approaches T_c the two-spin-wave peaks disappear into the tails of the single spin-wave peak and the diffusive central peak. For the ferromagnetic case the two-spin-wave peaks do not disappear entirely, the two-spin-wave peak corresponding to the lowest \mathbf{q} spin waves remains and the other two-spin-wave peaks broaden to disappear into its tail. A previous study by Chen *et al.* [6] misidentified the peak in the longitudinal component as a single spin-wave

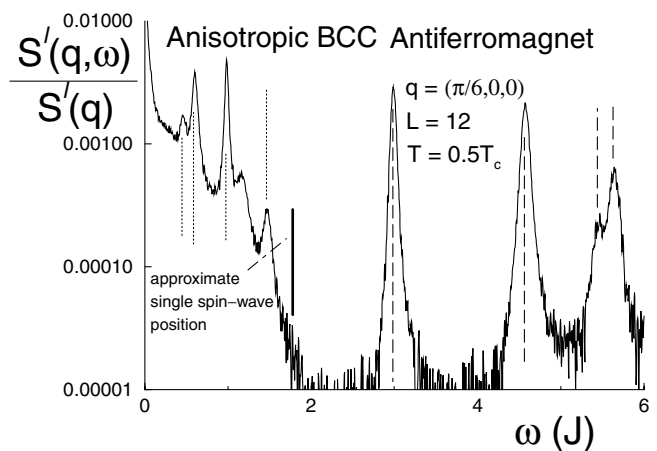


FIG. 2. The longitudinal component of the dynamic structure factor for the weakly anisotropic antiferromagnet, MnF_2 vs frequency. We compare the predicted positions of two-spin-wave peaks to the actual peak positions. The dotted lines are predicted positions of two-spin-wave annihilation peaks and the dashed lines are the predicted positions of two-spin-wave creation peaks. Note that once again we have used a logarithmic scale.

excitation. This happened because they were only able to look in the [100] lattice direction for which the dominant two-spin wave is at the same frequency as the single spin-wave peak for any given \mathbf{q} . Since for ferromagnets only spin-wave annihilation peaks are present, the dominant two-spin wave process found in the [100] direction is $[q, 0, 1] - [0, 0, -1]$. Since in the low \mathbf{q} limit $\omega \propto q^2$, $\omega([q, 0, 0]) \approx \omega([q, 0, 1]) - \omega([0, 0, -1])$. This is however not the case for the [111] direction. In Fig. 3 we show the longitudinal and transverse components in the [100] and [111] directions at temperatures approaching T_c . Note the fact that the longitudinal and transverse spin wave peaks are at the same frequency in the [100] direction but not in the [111] direction.

The existence of a set of finite two-spin-wave peaks is an artifact of the finite size of the lattice we use in our simulation. If one were to measure the longitudinal component of the dynamic structure factor for a real crystal, i.e., effectively an infinite lattice of magnetic moments, the spectrum

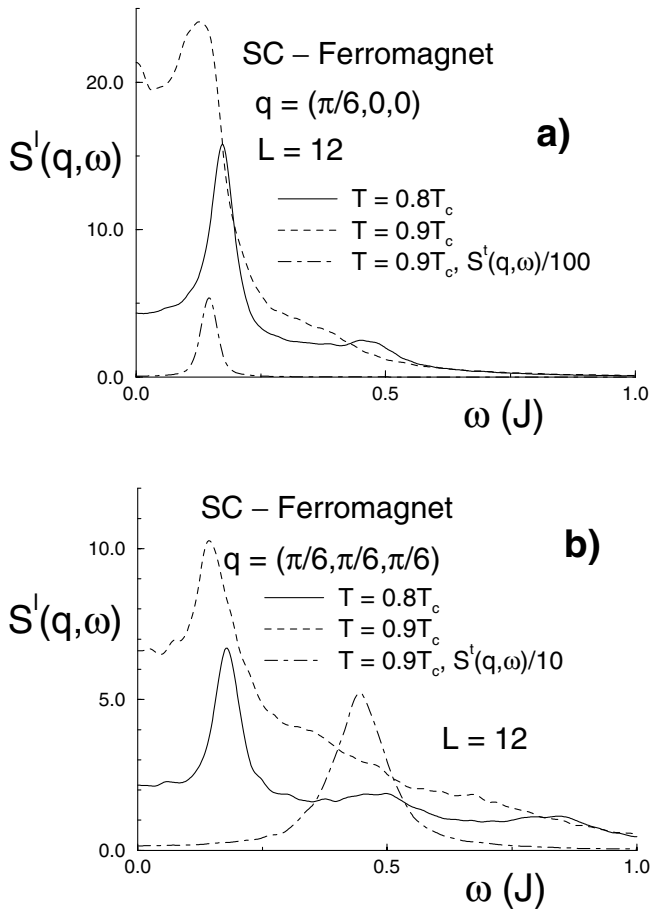


FIG. 3. The longitudinal and transverse components of the dynamic structure factor vs frequency as temperature approaches the critical regime are shown; (a) shows the [100] direction and (b) shows the [111] direction. A resolution function with coefficient $\delta_\omega = 0.01/|J|$ was used. The data are unnormalized to show the relative intensities of the longitudinal and transverse spin-wave peaks.

of possible two-spin-wave peaks would be continuous. The longitudinal component of the dynamic structure factor for the isotropic antiferromagnet has been measured experimentally by Cox *et al.* [5]. Taking measurements in the [111] direction, they found a diffusive central peak and a propagative spin-wave peak at the same frequency as the transverse single spin-wave peak. The longitudinal component of the dynamic structure factor for the isotropic ferromagnet EuO has been found experimentally to have a propagative spin wave and no diffusive central peak [4].

For both the ferro- and antiferromagnetic cases, the longitudinal excitations at the single spin-wave peak frequency can be explained in terms of two-spin-wave peaks as follows. Since spin-wave intensity increases with decreasing q the most intense two-spin waves will be those which are comprised of one spin wave with a very small q and another spin wave with a \mathbf{q} very close to the resultant two-spin wave \mathbf{q} . If we look at the limit of infinite lattice size, i.e., the real system, for the isotropic case a spin wave with extremely small q will have a negligible frequency. Thus the intensity of the two-spin-wave creation and annihilation peaks will have a maximum at the single spin-wave frequency. Even though only annihilation two-spin-wave peaks are present for the ferromagnetic case one should still see this effect in both the ferro- and antiferromagnetic cases and this is what is seen in the experiments [4,5]. We see no evidence of a diffusive central spin-wave peak in the longitudinal component of the dynamic structure factor for the isotropic ferromagnet in agreement with the experimental results of Dietrich *et al.* [4], and the theoretical result of Villain [11] but in disagreement with the theoretical predictions of Vaks *et al.* [2].

When we apply this same reasoning to the anisotropic antiferromagnet, which as shown in Fig. 2 also displays the same two-spin-wave peak behavior, we are left with an extremely intriguing result which can be measured experimentally. A spin wave at very small \mathbf{q} will no longer have a negligible frequency but instead the frequency of the energy gap at the Brillouin zone center. If our hypothesis about the origin of excitations in the longitudinal component of the dynamic structure factor is correct then for an anisotropic antiferromagnet one will observe an apparent splitting in the spin-wave peak in the longitudinal component. In an infinite lattice there will be a peak due to two-spin-wave creation which is shifted upwards from the single spin-wave frequency by an amount equal to the energy gap, and a spin-wave annihilation peak shifted downwards by the same frequency. While it is a very difficult experiment to perform, given a large enough crystal of MnF_2 , one could perform a polarization analysis and separate the transverse and longitudinal components of the spin excitations [12].

The theoretical explanation as to why the longitudinal component of the dynamic structure factor is made up of two-spin-wave peaks and why only two-spin-wave annihilation peaks are present for the ferromagnetic case while

both two-spin-wave annihilation and creation peaks are present for the antiferromagnetic case is as follows. If we express the dynamics in quantum mechanical formalism the spins, as they appear in the Hamiltonian, are expressed in terms of the operators \mathbf{S}_i^+ , \mathbf{S}_i^- , and \mathbf{S}_i^z where

$$\mathbf{S}_i^+ = \mathbf{S}_i^x + i\mathbf{S}_i^y, \quad (0.4)$$

$$\mathbf{S}_i^- = \mathbf{S}_i^x - i\mathbf{S}_i^y. \quad (0.5)$$

\mathbf{S}_i^+ and \mathbf{S}_i^- can be expressed in terms of ladder operators, a_i and a_i^\dagger , which raise or lower \mathbf{S}_i^z by one quanta. In the linear approximation

$$\mathbf{S}_i^+ = (2\mathbf{S})^{1/2} a_i^\dagger, \quad (0.6)$$

$$\mathbf{S}_i^- = (2\mathbf{S})^{1/2} a_i. \quad (0.7)$$

If we take the approximation for \mathbf{S}_i^z to one order higher than $\mathbf{S}_i^z = \mathbf{S}$ then

$$\mathbf{S}_i^z = \mathbf{S} - a_i^\dagger a_i = \mathbf{S} - \frac{1}{2\mathbf{S}} \mathbf{S}_i^+ \mathbf{S}_i^-. \quad (0.8)$$

For the classical limit this corresponds to an infinitesimal raising and lowering of the z component of the spin which is a longitudinal spin wave. These spin waves will be at the frequencies corresponding to the difference between the frequencies of single transverse spin waves since they result from creation followed by annihilation of a spin wave. Thus for the ferromagnetic case all two-spin-wave excitations will result from these annihilation processes. This result could probably be also obtained using an analytical spin-wave calculation, for example, possibly using the Holstein-Primakoff formalism [13], however such an analysis is beyond the scope of this paper.

Unlike the ferromagnetic the antiferromagnet is not a quantum state of the Heisenberg Hamiltonian. As a result the a_i and a_i^\dagger are replaced through a Bogoliubov transformation by new operators which are a linear combination of the creation and annihilation operators but which only connect excitations on the same sublattice [14]. As a result both creation and annihilation two-spin-wave excitations exist.

In conclusion, for magnets which can be described by a classical spin model, the longitudinal propagative excitations are made up of two-spin-wave peaks. In agreement with our theoretical picture only annihilation two-spin-wave peaks were present for the ferromagnetic case but both annihilation and creation two-spin-wave peaks are present for both the isotropic and anisotropic antiferromagnets. As the temperature approached the critical regime

the longitudinal two-spin-wave peaks broadened and converged into a single peak at the frequency of the dominant lowest- q two-spin-wave peak. In an isotropic lattice of infinite size, i.e., a real crystal, the two-spin waves will result in a peak at the single spin-wave frequency for either ferromagnetic or antiferromagnetic isotropic systems, in agreement with experimental results [4,5]. For the anisotropic antiferromagnet both creation and annihilation two-spin-wave peaks exist, and the longitudinal component of the anisotropic antiferromagnet should show two peaks; a two-spin-wave annihilation peak at the single spin-wave peak frequency minus the energy gap frequency, and a two-spin-wave creation peak at the single spin-wave peak frequency plus the energy gap frequency. This result indicates the presence of a new form of excitation behavior in magnetic materials which can be directly tested experimentally.

We thank Shan-Ho Tsai, Roderich Moessner, Werner Schweika, and Michael Krech for helpful suggestions and stimulating discussions. This research was supported in part by NSF Grant No. DMR9727714.

*Current address: Max Planck Institute for Polymer Research, Ackermann Weg 10, Mainz 55128, Germany.

- [1] U. Balucani and V. Tognetti, *Riv. Nuovo Cimento* **6**, 39 (1976).
- [2] V. G. Vaks, A. I. Larkin, and S. A. Pikin, *Sov. Phys. JETP* **26**, 647 (1968).
- [3] P. W. Mitchell, R. A. Cowley, and R. Pynn, *J. Phys. C* **17**, L875 (1984), and references therein.
- [4] O. W. Dietrich, J. Als-Nielsen, and L. Passell, *Phys. Rev. B* **14**, 4923 (1976).
- [5] U. J. Cox, R. A. Cowley, S. Bates, and L. D. Cussen, *J. Phys. Condens. Matter* **1**, 3031 (1989).
- [6] K. Chen and D. P. Landau, *Phys. Rev. B* **49**, 3266 (1994).
- [7] A. Bunker, K. Chen, and D. P. Landau, *Phys. Rev. B* **54**, 9259 (1996).
- [8] K. Binder, *Phys. Rev. Lett.* **47**, 693 (1981).
- [9] K. Chen, A. M. Ferrenberg, and D. P. Landau, *Phys. Rev. B* **48**, 3249 (1993).
- [10] J. Als-Nielsen, in *Phase Transitions and Critical Phenomena 5A*, edited by C. Domb and M. S. Green (Academic Press, New York, 1976).
- [11] J. Villain, in *Critical Phenomena in Alloys, Magnets and Superconductors*, edited by R. E. Millis, E. Asher, and R. I. Jaffee (McGraw-Hill, New York, 1971), p. 423.
- [12] W. Schweika (private communication).
- [13] C. Kittel, *Quantum Theory of Solids* (John Wiley & Sons, New York, 1963).
- [14] D. C. Mattis, *The Theory of Magnetism I: Statics and Dynamics*, Springer Series in Solid-State Science Vol. 17 (Springer-Verlag, Berlin, 1988).